International Journal of Thermophysics, Vol. 28, No. 5, October 2007 (© 2007)
DOI: 10.1007/s10765-007-0155-5

Thermophysical Analysis of Gioia Marble in Dry and Water-Saturated States by the Pulse Transient Method[1]

V. Vretenár,[2,3] Ľ. Kubičár,[2] V. Boháč,[2] and P. Tiano[4]

Measurements of the thermophysical properties of Gioia marble in the temperature range from −20 to 60°C are presented. Thermophysical properties, namely, thermal diffusivity, thermal conductivity, and specific heat, were measured by the pulse transient technique. The data were compared for dry and water-saturated states. Despite the very low porosity of marble of about 0.6 vol%, an increase of the transport property parameters (thermal diffusivity and thermal conductivity) up to 20% after water saturation was found. To verify the differences in the transport parameters, the ultrasonic pulse velocity method was employed. A detailed analysis of thermophysical property data during the freeze/thaw process for dry and water-saturated marble was carried out in the temperature range from −8 to 1°C, where an anomaly in the water freezing process was observed. In order to study artificial aging of Gioia marble, up to 60 freeze/thaw cycles were performed. No significant changes in the thermophysical properties of Gioia marble were observed during the artificial aging process.

KEY WORDS: freeze/thaw cycle; marble; porosity; pulse transient technique; specific heat; thermal conductivity; thermal diffusivity; ultrasonic pulse velocity.

[1] Paper presented at the Seventeenth European Conference on Thermophysical Properties, September 5–8, 2005, Bratislava, Slovak Republic.

[2] Institute of Physics, Slovak Academy of Sciences, Dúbravská cesta 9, 845 11 Bratislava, Slovak Republic.
[3] To whom correspondence should be addressed. E-mail: fyzivili@savba.sk
[4] CNR-ICVBC, Edificio C, 50019 Sesto Fiorentino, FI, Italy.

1. INTRODUCTION

Stones are porous materials where water in pores significantly influences material properties and plays an important role in material durability during freeze–thaw processes [1,2]. Variations of thermophysical properties based on moisture content depend on both skeleton and pore properties, particularly on the skeleton structure, pore shapes and pore-size distribution, size of open porosity, etc. Therefore, thermophysical property measurements become a suitable tool to characterize porous materials.

A number of experimental methods have been developed to investigate heat transport through porous structures. Generally they can be divided into two groups, namely, methods that use a steady-state measuring regime [3] and methods using a transient one [4]. The first of these methods needs a long measuring time which, for the case of porous structures, can induce redistribution of the fluid inside the pores and thus the information is obtained at conditions far from the desired measuring conditions. Transient methods need significantly shorter measuring times and thus the information is obtained at conditions close to those found in real applications.

In this paper we present measurements of thermophysical and elastic properties of Gioia marble, namely, thermal diffusivity, specific heat, and thermal conductivity, in the temperature range from -20 to 60°C, using the pulse transient method [5] and the modulus of elasticity at room temperature using the ultrasonic pulse velocity method [6]. The specimen, Gioia marble, was conditioned to obtain dry and water-saturated states. Apart from a standard measuring procedure, a non-isothermal measuring regime in the temperature range from -8 to 1°C using a cooling and heating rate of $0.01\,\mathrm{K\cdot min^{-1}}$ was used in order to analyze the freeze–thaw process. Due to low cooling and heating rates and the specimen temperature control from opposite specimen faces, we assume that thermodynamic equilibrium has been maintained during the cooling and heating regimes. Up to 60 freeze–thaw cycles that might induce structural damage in stone skeleton were used to obtain a picture of material degradation and its durability.

2. EXPERIMENTAL METHODS

The major part of measurements was carried out with the pulse transient method, whereby we carried out the thermophysical property investigations of marble specimens. To verify unexpected behavior of thermal diffusivity and thermal conductivity, we used another related method. Since the elasticity is closely related to the thermal diffusivity and thermal conductivity by dynamical properties of materials, we employed a

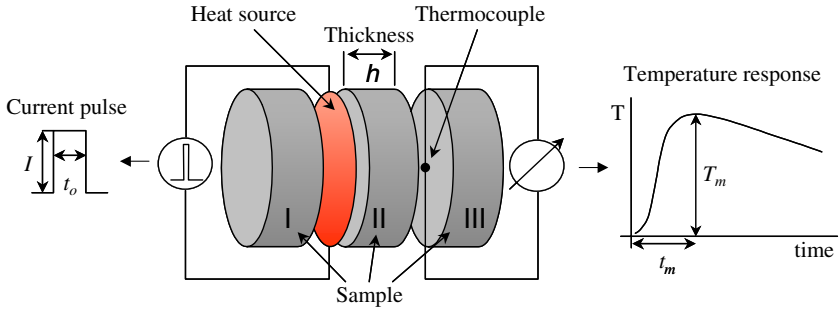

Fig. 1. Experimental setup for the pulse transient method.

measurement of the modulus of elasticity by the ultrasonic pulse velocity method.

2.1. Pulse Transient Method

2.1.1. Theory

The principle of the pulse transient method [5] is shown in Fig. 1. The specimen consists of three parts (I, II, III). A planar heat source is clamped between the first and second parts. The heat pulse is produced due to Joule heating from the electrical resistance of the planar source. One junction of a thermocouple is placed between the second and third parts, where the temperature of the second junction is stabilized. The method can be described as follows. The temperature of the specimen is stabilized and uniform. Then a small disturbance in the form of a heat pulse is applied to the specimen. The thermophysical properties are determined based upon the temperature response according to the model used.

The model of the method is characterized by the temperature function [5]

$$T(h,t) = \frac{2q}{c_p \rho \sqrt{a}} \left\{ \sqrt{t} \times i\Phi^* \left(\frac{h}{2\sqrt{at}} \right) - \sqrt{t-t_0} \times i\Phi^* \left(\frac{h}{2\sqrt{a\,(t-t_0)}} \right) \right\},$$

$$i\Phi^*(x) = \frac{1}{\sqrt{\pi}} \exp(-x^2) - x\Phi^*(x), \tag{1}$$

where $q = RI^2$ represents the heat flux supplied by the heat source per unit area, R is the electrical resistance of the heat source, I is the current supplied at time t_0, t is the time, h is the distance between the heat source and the temperature sensor, ρ is the specimen density, and a and c_p are the thermal diffusivity and specific heat, respectively. The symbol Φ^* denotes

a complementary error function. The temperature function in Eq. (1) is a solution of the heat equation considering appropriate boundary and initial conditions. To determine the thermophysical properties using the one-point procedure, the maximum of the temperature response is taken as the input. Then, the following relations [5] are used for calculation of the thermophysical properties:

Thermal diffusivity a

$$a = h^2 \Big/ (2 t_{\mathrm{m}} f_{\mathrm{a}}), \tag{2}$$

specific heat c_p

$$c_p = f_{\mathrm{c}} q \Big/ \sqrt{2\pi e}\, \rho h T_{\mathrm{m}}, \tag{3}$$

where T_{m} represents the maximum temperature response at the time t_{m} and e denotes the Euler number. The coefficients f_{a} and f_{c} are defined by $p = t_{\mathrm{m}}/t_0$ as

$$f_{\mathrm{a}} = (p-1) \ln\left(\frac{p}{p-1}\right) \tag{4}$$

$$f_{\mathrm{c}} = 2\sqrt{\pi e f_{\mathrm{a}}}\, p \left\{ \frac{1}{\sqrt{\pi}} \left[\exp\left(-\frac{f_{\mathrm{a}}}{2}\right) - \sqrt{\frac{p-1}{p}} \exp\left(\frac{-p f_{\mathrm{a}}}{2(p-1)}\right) \right] - \sqrt{\frac{f_{\mathrm{a}}}{2}} \left[\Phi^*\left(\sqrt{\frac{f_{\mathrm{a}}}{2}}\right) - \Phi^*\left(\sqrt{\frac{p f_{\mathrm{a}}}{2\,(p-1)}}\right) \right] \right\}. \tag{5}$$

The third thermophysical property, thermal conductivity λ, is defined by the well-known relation

$$\lambda = a c_p \rho. \tag{6}$$

The thermophysical properties can be also found by superimposing the temperature function, Eq. (1), on the temperature response using an appropriate fitting technique.

2.1.2. Experimental Setup

The instrument RTB 1.01 (Institute of Physics SAS) is used for measuring the thermophysical properties. A basic schematic diagram of the instrument is shown in Fig. 2. The thermostat in combination with the plate heat exchangers establishes the specimen temperature. Both a non-isothermal measuring regime with a heating and cooling rate of

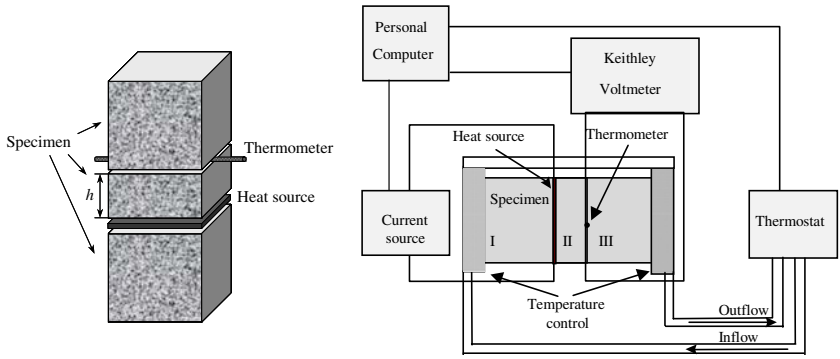

Fig. 2. Specimen setup (left) and basic scheme of instrument RTB 1.01 (right).

$0.01\,\mathrm{K{\cdot}min^{-1}}$ and an isothermal regime within the limit of 0.02 K were used. A programmable current source was used for generation of a heat pulse using a planar electrical resistance of $2\,\Omega$. The planar heat source was made of nickel foil of $20\,\mu$m thickness etched in the form of a meander and covered from both sides in Kapton foil of $25\,\mu$m thickness. The temperature response was scanned with a Keithly multimeter. A pc computer synchronizes all units. The typical parameters of the temperature response were $T_m \sim 1\,\mathrm{K}$ and $t_m \sim 120\,\mathrm{s}$.

The sample was prepared in the form of three blocks with a cross-section of $50 \times 50\,\mathrm{mm^2}$, where the thickness of the measured active middle part of the specimen setup (h) was 14.6 mm. In order to provide good thermal contact between the individual parts of the specimen, a thermal paste was used. Since the sample is porous, the contact specimen surfaces were treated with an epoxy layer. Values of overall uncertainties, estimated from a one-point evaluation procedure, were up to 6% for the thermal diffusivity and up to 4% for the specific heat and thermal conductivity [7].

2.2. Ultrasonic Pulse Velocity Method

2.2.1. Theory

A simple sketch of the ultrasonic pulse velocity method is depicted in Fig. 3. The method is based [6] on a velocity measurement of the propagation of elastic vibration in solids. On one side of the sample, supported by a small base, the frequency generator produces pulses to the ultrasonic exciter, which converts them into elastic vibration spreading along the sample. On the other side of the sample, the ultrasonic sensor records the response. From the time shift of the pulses and from the distance

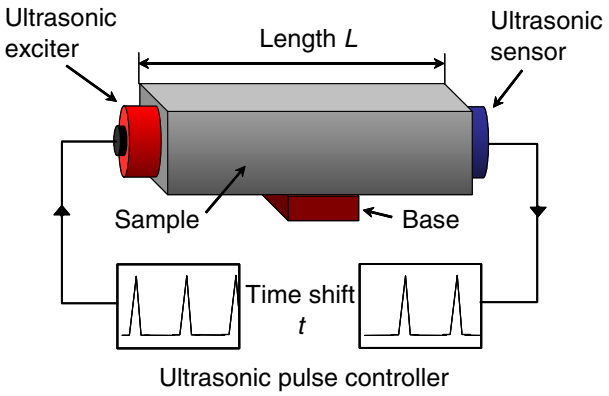

Fig. 3. Experimental arrangement of the ultrasonic pulse transient method.

between the ultrasonic source and the sensor, the modulus of elasticity E is calculated using the following simple equation derived for a one-dimensional homogenous isotropic solid [6]

$$E = \rho \left(\frac{L}{t} \right)^2, \tag{7}$$

where L represents the length of the sample, ρ is the density of the sample, and t is the time of pulse propagation through the sample.

2.3. Experimental Setup

A complete measurement system, Ultrachall-messgerät USME-D (Geotron), is used to determine the ultrasonic pulse velocity through the sample in accordance with STN 731371, ASTM C 597-83(91) "Method for ultrasonic pulse testing of concrete." The measurement device has an electromagnetic ultrasonic exciter UNG working at a frequency of 150 kHz and a piezoelectric ultrasonic sensor VPE. The measurements were performed on a sample stabilized at room temperature in atmospheric air.

The sample was prepared in the form of a prism with a cross-section of $50 \times 50\,\text{mm}^2$ and a length of 100 mm. To achieve some sonic contact between the measurement device and the sample, both the ultrasonic exciter and the ultrasonic sensor were treated with lubricating grease. The primary contribution to the overall uncertainty estimated for the modulus of elasticity originates from the uncertainty of the time assessment of up to 5%.

3. SAMPLE CHARACTERIZATION

The sample was cut from marble from the Gioia quarry in Carrara, Italy. Homoblastic Gioia marble belongs to calcite marble with a typical granoblastic polygonal microstructure (see Fig. 4). Since it does not show any preferential orientation, it is considered to belong to isotropic porous rocks. Marble has very low, mainly open porosity as seen in basic characteristics reported in Table I. The calculated water porosity (only 0.6 vol%) was obtained from the difference between the densities for dry and water-saturated states. The water absorption by capillary action is of adequate value for such a low-porosity material.

The pore-size distribution of marble depicted in Fig. 5 shows remarkably strong nano-porosity around 60 nm. It is necessary to note that the nano-porosity and the pore-size distribution found in marble is a common feature of many stones. In addition to the size, the shape of pores plays a key role in changes in the transport physical properties of stones after water saturation. A detailed look at the Gioia microstructure (Fig. 4, right) shows the pores at the boundaries of grains in the form of capillaries (usually named veins) or flat capillaries. This is a unique property of marble that distinguishes it from other stones [2].

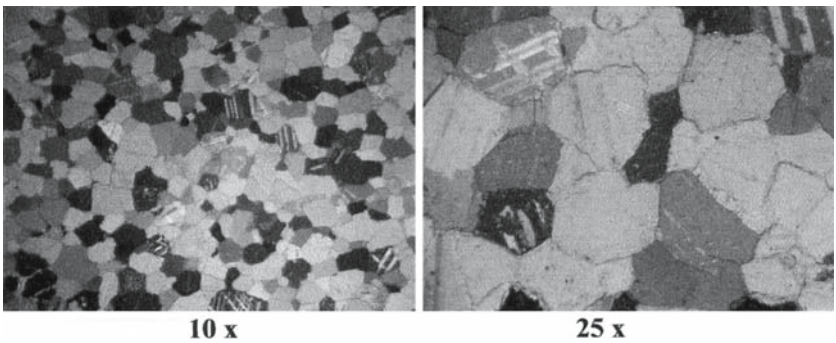

Fig. 4. SEM images of microstructure of Gioia marble.

Table I. Basic Characteristics of Gioia Marble

Density ($kg \cdot m^{-3}$)		Water porosity (%)		Water absorption by capillarity ($kg \cdot m^{-2} \cdot h^{-0.5}$)
Dry	Water-saturated	Calculated	Published	
2703 ± 3	2710 ± 3	0.65 ± 0.3	0.3 ± 0.0	$(3.2-6.0) \times 10^{-2}$

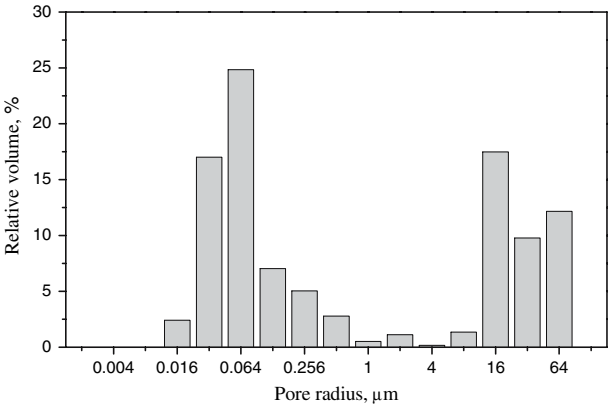

Fig. 5. Pore-size distribution of Gioia marble.

The dry state was reached within a drying cycle at 60°C for 2 h, followed by reweighing at 25°C. Cycling was repeated until the limit in the mass change between two consecutive cycles was less then 0.1%. The water-saturated state was reached by immersing the specimen into distilled water for 2 h, followed by reweighing. This cycle was repeated until the mass change between two consecutive weighings was less than 0.3%.

4. EXPERIMENTAL DATA AND DISCUSSION

Figure 6 depicts the dependence of the thermophysical properties of dry Gioia marble on temperature in the range from −20 to 60°C. The thermal diffusivity, specific heat, and thermal conductivity are plotted as a function of temperature. The large scatter of thermophysical property data above 50°C is caused by insufficient thermal insulation of the measuring apparatus from the surroundings. It is evident that the decrease of the thermal diffusivity and thermal conductivity with temperature is related to the polycrystalline structure of Gioia marble.

Data on the thermophysical properties for dry and water-saturated marble in the temperature range from −8 to 1°C are shown in Fig. 7. The measuring process of the thermophysical properties during the freeze/thaw process consists of subsequent cooling and heating regimes. As expected, the behavior of the thermophysical properties of dry marble is identical for both the cooling and heating regimes. Therefore, for the sake of clarity, only the curves corresponding to the cooling regime are depicted in Fig. 7 for dry marble.

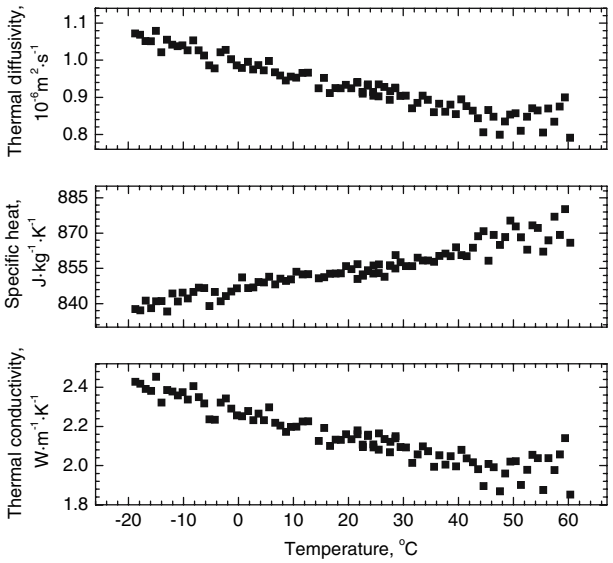

Fig. 6. Thermophysical properties of dry Gioia marble as a function of temperature.

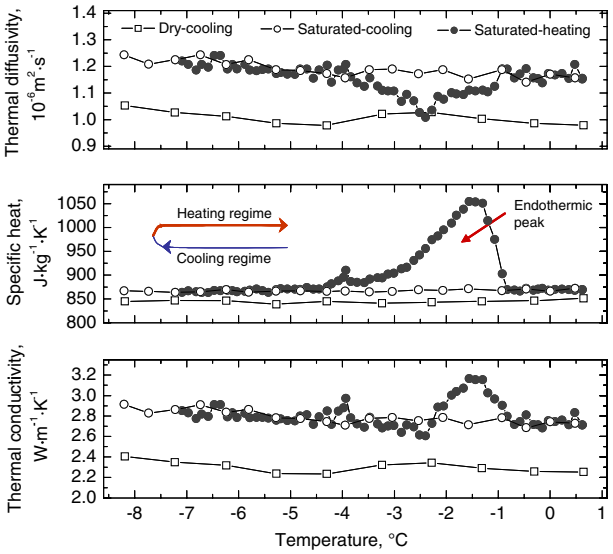

Fig. 7. Thermophysical properties of dry and water-saturated Gioia marble as a function of temperature during cooling and heating regimes.

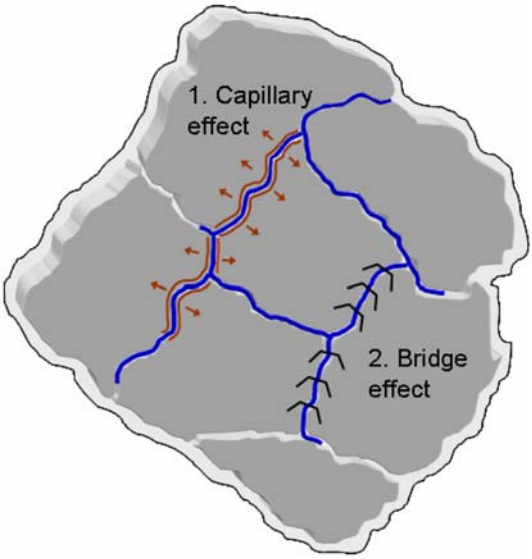

Fig. 8. Porosity model of Gioia marble—effects of moisturizing.

Anomalies of the thermophysical properties were found for the water-saturated state, where the endothermic peaks associated with the phase transition of ice water were observed just for the heating regime. The energy of heat pulses applied to the sample during measurements is depleted by the phase transition of ice water resulting in increased values of the specific heat. Of course, the values of thermophysical properties in the region of the endothermic peaks do not correspond to real values of Gioia marble, because the physical model used for evaluation of measured data does not consider the phase transitions. The solidification (freezing) phenomenon is a complicated function of the droplet size—pore volume and its interaction with the pore surface. Thermodynamics of the pore content determine embryo formation and solid-phase growth. Since Gioia marble has a very strong nano-porosity (seen in Fig. 4) and pore occurrence in the form of veins [2] (Fig. 5), the creation of the solid phase (ice) in the pore volume is assumed to be shifted to lower temperatures, a few °C below zero, as a result of high capillarity forces inside the pores. The capillary effect in marble is illustrated in Fig. 8. In such a situation the water below 0°C is characterized as an under-cooled liquid. As the temperature is decreased, the increasing solid phases of water inside the pores immediately reach a "deep" frozen state, where the heat pulses supplied during the measuring procedure are of insufficient energy to start the

Table II. Thermophysical Properties of Gioia Marble for Dry and Water-Saturated States

	−6°C			0.5°C		
Parameter	Dry	Water-saturated	Diff.	Dry	Water-saturated	Diff.
Thermal diffusivity ($10^{-6}\,m^2 \cdot s^{-1}$)	1.012	1.191	18%	0.979	1.177	20%
Specific heat ($J \cdot kg^{-1} \cdot K^{-1}$)	846.6	865.2	2%	851.1	867.9	2%
Thermal conductivity ($W \cdot m^{-1} \cdot K^{-1}$)	2.32	2.78	20%	2.25	2.75	22%

reverse thawing process. Therefore, no peaks related to the phase transition of ice water were observed during the cooling regime, as seen in Fig. 7. On the contrary, the heating regime starts from a temperature of −10°C, where water in pores is completely frozen and capable of a phase transition.

Differences in the thermophysical properties for dry and saturated states at −6°C (water in pores is frozen) and at 0.5°C are reported in Table II. While a difference in the specific heat for the dry and water-saturated states is around 2% which corresponds to a low porosity, significantly larger differences of about 20% exist in values of the transport properties, the thermal diffusivity and thermal conductivity, for both temperatures of −6°C and 0.5°C.

Usually a stone skeleton plays a significant role in heat transport while the role of the pore content is negligible. The thermal diffusivity is a function of the sound speed and free path of phonons [8]. Data for the thermal diffusivity and related thermal conductivity indicate that elastic properties of the stone are influenced by moisture content. As already stated, this is supposed to be due to high capillarity forces, the "capillary effect," inside the wet stone, wherein they enhance the tension of the whole structure and increase the elastic properties. In addition, a simple mechanism, the "bridge effect," where water in capillaries simply connects the isolated sides of grains, improves the transport properties (see Fig. 8). On the contrary to thermal diffusivity, data on the specific heat indicate that the thermodynamic properties of the stone are influenced by the volume of the pores and its content. Thus, the change of the specific heat is very small, taking into account the stone's porosity. The thermal conductivity, as a product of thermal diffusivity and specific heat (Eq. (6)), simply follows the variation of thermal diffusivity.

To verify the relatively enormous increase of the thermal diffusivity and thermal conductivity, the elastic properties of Gioia marble were

Table III. Modulus of Elasticity E of Gioia Marble for Dry and Water-Saturated States

		Dry		Water-saturated	
Cross-section (mm^2)	Length (mm)	Time (μs)	E (GPa)	Time (μs)	E (GPa)
50×50	100	24.2	44.8	20.2	64.6

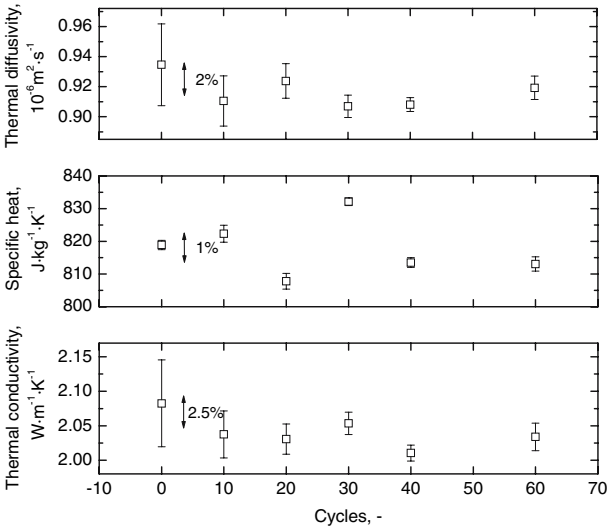

Fig. 9. Artificial aging of Gioia marble (dependence of thermophysical properties on number of freeze/thaw cycles).

determined. The modulus of elasticity E for dry and water-saturated states was measured by the ultrasonic pulse velocity method. Data are reported in Table III. The increase of the modulus of elasticity of Gioia marble after water saturation was about 44%, which exceeded our expectations considering the changes of thermophysical properties. Nevertheless, the result is consistent with the measurements performed with the pulse transient method.

The volume change during freezing of water induces damage of the stone skeleton. It is believed that the pore distribution is changed and heat-conducting paths are interrupted [9, 10]. Therefore, cycling experiments, where water-saturated Gioia marble underwent freeze–thaw processes, were performed. A freezing box at $-18°C$ and a room temperature box at $25°C$

were used for the freeze–thaw cycle. The water-saturated specimen was alternatively placed into the freezing box and the room temperature box, each for 6 h, to induce an artificial aging cycle. Typically, 10 artificial aging cycles were performed. Then a drying procedure was realized, followed by measurements of the thermophysical properties. The results are shown in Fig. 9 where the properties are plotted as a function of the cycle number. All measurements were carried out on a dry sample at room temperature. Over the duration of 60 freeze/thaw cycles, no significant changes in thermophysical properties of marble Gioia were observed, which suggests its good stability. Probably, there are no destructive changes of the pores during freezing. A similar artificial aging test was performed on Sander sandstone, where structural changes occurred within 20 cycles [7].

The thermophysical properties of moist porous materials are strongly affected by both the moisture distribution and moisture transport induced by heat flow inside the inspected material, which results in the concept of apparent values [11]. Since cooling and heating rates of $0.01\,\mathrm{K\cdot min^{-1}}$ were used, we assumed a homogenous moisture distribution inside the specimen before each measurement. Redistribution of the moisture could be initiated by the heat pulses supplied during the individual measurements. However, considering the dimensions of the specimen, the process of moisture redistribution corresponds to time periods quantified in hours [11, 12], which is in contrast to very short measuring times (about 120 s) used in the pulse transient technique. Due to this, a complex model of heat and moisture transport was not taken into consideration.

5. CONCLUSIONS

The thermophysical properties of Gioia marble were measured by the pulse transient method in the temperature range from -20 up to 60°C. An analysis was performed for both dry and water-saturated states, while the freeze/thaw process was applied in the temperature range from -8 to 1°C.

Two peculiarities in the thermophysical behavior of Gioia marble were found, an anomaly of water freezing inside the marble during the freeze/thaw process and a significant increase of the transport properties (relative to nearly zero porosity) after the marble was water saturated. In order to explain both observed peculiarities, the theory of high capillarity forces (capillary effect) inside the water-saturated marble was proposed. In the first case, high capillarity forces inside the pores prevent the water from freezing, which induces a state of under-cooled liquid flipping to a "deep" frozen state at lower temperatures. In the second case, the high capillarity forces increase the elastic properties of the marble skeleton

and, along with the bridge effect, this results in an enhancement of the transport properties of Gioia marble.

No significant damage of homoblastic marble Gioia was observed within 60 cycles of the freeze/thaw process during an artificial aging test. The measurements of thermophysical properties on Gioia marble unequivocally showed the significant influence of the moisture content inside the stones, even for very low porosities.

ACKNOWLEDGMENTS

This research was carried out under the EU project "MCDUR: Effects of the weathering on stone materials: Assessment of their Mechanical Durability" under Contract G6RD-CT2000-00266. The experimental technique was partly financially supported by project VEGA under Contract No.: 2/2036/22. The authors are thankful for permitting to use data in Fig. 5, measured by M. Montoto, and for the ultrasonic pulse velocity measurements, carried out by Ľ. Bágeľ, ICA SAS.

REFERENCES

1. Y. C. Yortsos and A. K. Stubos, *Curr. Opin. Colloid Interface Sci.* **6**:208 (2001).
2. M. Montoto, in *Publicación Técnica* (Enresa, Madrid, 2003), p. 297.
3. K. D. Maglić, A. Cezairliyan, and V. E. Peletsky, eds., in *Compendium of Thermophysical Property Measurement Methods*, *Vol. 2*, *Recommended Measurement Techniques and Practices* (Plenum Press, New York and London, 1992), p. 643.
4. Ľ. Kubičár and V. Boháč, in *Proc. 24th Int. Conf. on Thermal Conductivity/12th Int. Thermal Expansion Symp*, P. S. Gaal and D. E. Apostolescu, eds. (Technomic Pub. Co., Lancaster, Pensylvania, 1999), pp. 135–149.
5. Ľ. Kubičár, in *Comprehensive Analytical Chemistry*, G. Svehla, ed. (Elsevier, Amsterdam, Tokyo, Oxford, New York, 1990), p. 360.
6. G. Martinček, in *Non-destructive Dynamic Methods for Building Materials and Constructions Testing*, J. Stork, ed. (Slovak Academy of Sciences, Bratislava, 1962), p. 242. [in Slovak]
7. Ľ. Kubičár, V. Vretenár, V. Boháč, and P. Tiano, *Int. J. Thermophys.* **27**:220 (2006).
8. G. Grimvall, in *Selected Topics in Solid State Physics*, E. P. Wohlfarth, ed. (North-Holland, Amsterdam, 1968), Vol. XVIII, p. 345.
9. T. Popp and H. Kern, *Phys. Chem. Earth* **23**:373 (1998).
10. K. Ivanova, *Eur. Phys. J. B* **15**:327 (2000).
11. S. Rudtsch, *High Temp. High Press.* **32**:487 (2000).
12. O. Koronthalyova and P. Matiasovsky, *J. Therm. Envel. Build. Sci.* **27**:71 (2003).